A non-contact impedimetric biosensing system for classification of toxins associated with cytotoxicity testing.

Angelines Gasser, John Eveness*, Janice Kiely, David Attwood, Richard Luxton

University of the West of England, Institute of Bio-Sensing Technology
Bristol, BS16 1QY, U.K.
*Corresponding author. Tel.: +44(0)117 32 87667; e-mail: john.eveness@uwe.ac.uk).

Abstract

We report on a novel impedance spectroscopy measurement and data analysis technique for cytotoxicity testing. The technique combines non-contact measurement with real-time impedance data analysis based on the toxin dose dependency of the outputs, making it suitable for high throughput screening. A multi-electrode array was designed and fabricated such that a standard well plate could be positioned above the electrodes, negating the requirement for bespoke culture wells with integrated electrodes. For cytotoxicity testing, endothelial cells, type ECV304, within the wells were exposed to various concentrations of 3 toxins, dimethyl sulphoxide, cadmium chloride and saponin, which exhibit different modes of action on cells. Impedance spectra were recorded every 30 minutes over a 24 hour period. From the spectra 'toxin maps' were produced which presented the correlation between impedance output and dose of toxin versus frequency and time. The results demonstrated characteristic toxin maps for each toxin and significantly differences between the three toxins studied. Using complementary measurement methods, we showed that these differences in toxin maps related to morphological and physiological changes in the cells due to the differing mode of action of each toxin.

Keywords —Electrical-impedance-spectroscopy, cellular toxicity, toxin maps.

1.0 Introduction

Impedance measurement of live biological cells is widely accepted as an effective label-free, non-invasive and quantitative analytical method to assess cell status. The integration with other techniques, the fabrication of devices for biological assays and the development of point-of-need diagnostic devices are predicted to be the future trends for impedance sensing techniques due to their ease-of-use, low cost and flexibility [1]. Electric cell–substrate impedance sensing (ECIS) is a technique used to monitor cell status and behaviour by measuring the impedance of cells growing on electrodes within culture medium. Benefiting from the advantages that impedance based measurement offers, ECIS cell chips also combine flexibility with the ability to integrate a sensor and the associated circuitry. ECIS devices have been used to study the in-vitro response of cells to toxins [2, 3, 4] and to nanoparticles [5]. Impedance spectroscopy is equally suited to measurement of changes in the cell monolayer such as [6], proliferation [7], cell viability [3], cell

rity [11].

The adoption of high throughput screening (HTS) and high content analysis (HCA) for toxicity testing or drug discovery [12] allows for the testing of numerous materials, including chemicals and nano-materials [13], at different concentrations. HTS/HCA approaches facilitate the classification of key biological indicators of materials–cell interaction and are needed to assess dose and time dependent toxicity, allowing predication of in-vivo adverse effects. Traditionally, colorimetric or fluorometric endpoints are used to determine cytotoxic effects and a LD50 (a measure of the lethal dose) for a toxin, for example the Neutral Red Uptake Assay [14]. Impedance based sensing methods offer non-invasive alternatives that lend

themselves well to the demand of HTS.

Complementing impedance spectroscopy with appropriate signal post-processing can improve the assessment and quantification of a particular cellular response. Various techniques have been used to analyse bio-impedance signals. In particular, alteration of cell micro-motion and cell differentiation have been detected [6, 8] using De-trending Fluctuation Analysis and by performing moving variance analysis on the time-series impedance data [15]. This post-processing data analysis allows gradual changes in cellular dynamics and morphology to be quantified in a concentration dependent manner. Wavelet-based analysis has been applied to time-series impedance data measured at 40 kHz to evaluate the 'aggressiveness' of cancer cells [7], particularly identifying the micro-motions, growth dynamics and energy usage for cellular activity. A method of applying wavelet packet decomposition (WPD) to analyse impedance results of cytotoxicity testing has been investigated [16]. Since it is an appropriate technique to extract low and high frequency components from bio impedance signals it could be used to differentiate between intra- and inter-cellular changes. It was demonstrated that the WPD is an accurate technique for monitoring changes in cell morphology following a toxic challenge. Other signal processing techniques like Fast Fourier Transform (FFT) analysis have been applied to impedance data to analyse spontaneous cellular oscillations [17]. The Hilbert-Huang Transformation (HHT) has been investigated to deal with the non-linear and non-stationary nature of impedance signals and as a method to extract characteristic information from the data related to morphological changes during cytotoxicity testing [18, 19]. An impedance measurement system has been described for monitoring the response of ECV304 cells to two toxicants (dimethyl sulphoxide (DMSO) and sodium butyrate) [20]. The cell response for each toxin dose was plotted as a 3-D impedance spectra (impedance versus frequency and time) for each toxin concentration and compared with images of the cells. Changes in the characteristics of the impedance spectra with time and toxin concentration were shown to correlate with the morphological changes of cells. The techniques described above all provide useful methods for analysing impedance spectra and identifying changes in cells due to a toxic challenge. However, they do not make use of the information relating impedance data variation with toxin concentration, to permit rapid identification of a particular class of toxins.

In this paper we present a novel ECIS technique that involves a transformation of 3D impedance spectra data, utilising a measure of the correlation between toxin concentration and impedance output to generate a 'toxin map'. The toxin maps provide finger-print signatures of the cells' response to a toxic challenge. In this study, we investigated the cytotoxicity effects of dimethyl sulfoxide (DMSO), cadmium chloride and saponin on endothelial cells (type ECV304), comparing the toxin maps for each compound with morphological/physiological changes of the cells due to the effects of these toxins. These toxins were selected for the following reasons: they were readily available, they are not associated with excessive hazards and they have well defined and different effects on cells. DMSO is a potent cell differentiating agent and has marked effects on the growth, morphology and metabolism of cells. Cadmium chloride has more specific effects, acting as a potassium channel blocker and replacing calcium in Ca^{2+} binding proteins. Saponin is a potent membrane permeabilizing agent. In parallel with the impedance spectroscopy study, an analysis of cell morphological/physiological changes induced by the three toxins was undertaken using phase contrast microscopy and measurement of the release of lactate dehydrogenase (LDH). Changes in cell size were determined from microscope images and damage to the cell membrane from the released LDH in the cell culture media.

2.0 Materials and methods

2.1 Non-contact impedance Spectroscopy using an 8-Electrode System

The impedance analyser system, shown in Fig. 1(A), comprises 8 electrode pairs (figure 1B) and a signal phase-shift detector circuit (figure 1(C)) to measure changes in cell impedance. The method is non-invasive with a standard 12 well plate, containing the cells, being positioned on top of the electrodes during measurement, as shown in figure 1(A). This technique uses an array of 8 D-shaped electrode pairs of 22.1 mm diameter, which were fabricated on a printed circuit board (PCB). D-shaped electrodes, as shown in figure 1B, were selected for this study, as previous experimentation has demonstrated that this design had greater sensitivity than other designs, such as interdigitated and spiral patterns [21, 22].During impedance measurement each electrode was monitored independently and in sequence. One well was designated as the control and, during measurement, contained cells with no added toxicant.
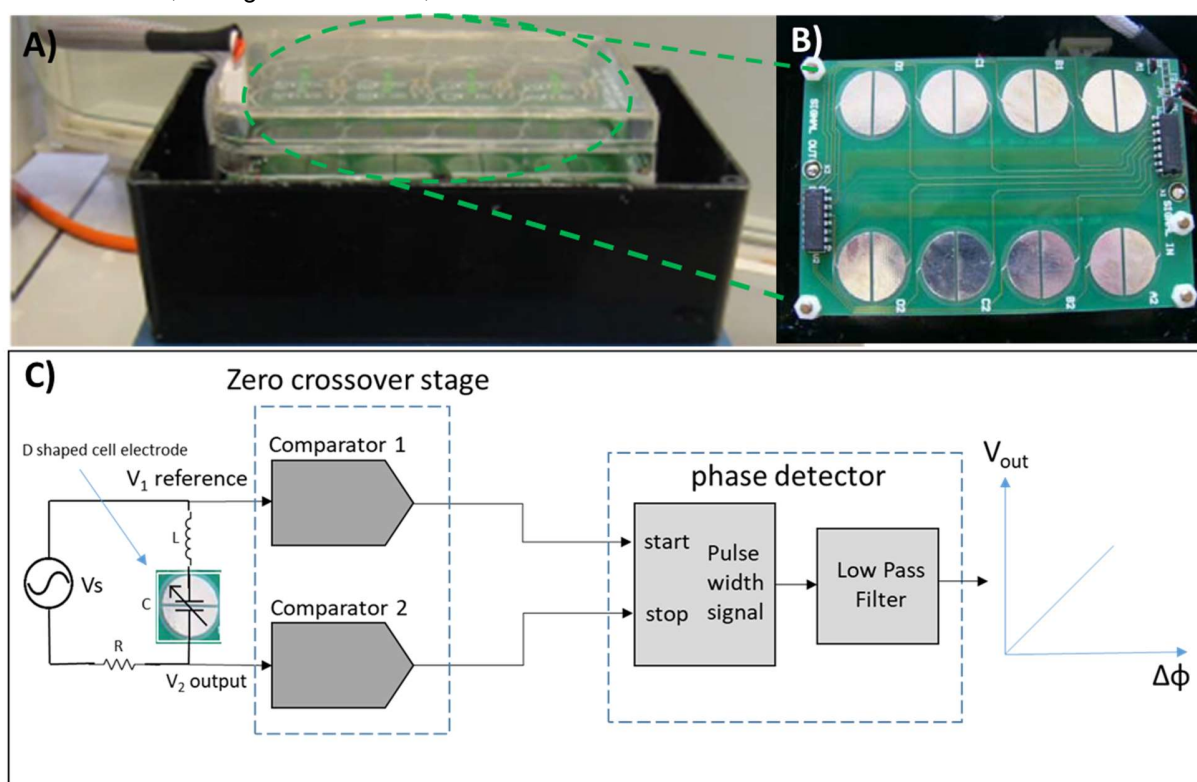

Fig. 1. Impedance analyser setup: A) the impedance analyser connected to a printed circuit board with an array of 8 electrodes which a 12 well plate is laid B) 8 electrode array PCB design C) schematic of the impedance analyser's phase shift detector circuit.

In a simple model of this ECIS system, the sensing electrode and cells form the capacitive reactance (X_c) element of a series resonant circuit, where the resonant frequency is set to approximately 2 MHz by suitable choice of fixed inductor (X_L). The frequency of the resonant circuit is swept from 400 to 2400 kHz at a sampling frequency of 10 kHz. The frequency sweep range is wide in order to capture impedance changes below and above resonance, to evaluate various aspects of the morphology/physiology of the cells. At resonance X_L and X_C are equal and cancel, thus the phase angle of the impedance is zero.

The impedance parameter recorded in this work is based on the change of phase angle (ϕ) between the input drive signal across the series resonant circuit and output signal across X_c and X_L. A block diagram of the circuit to produce the output voltage representing the phase angle change is shown in figure 1C. The phase angle is measured by converting the time difference between the zero crossing point of the input

(reference) voltage waveform (V_1) and the zero crossing point of the output waveform (V_2) into a single pulse and then determining the voltage corresponding to the phase angle change from the width of this pulse. The phase angle (ϕ) in radians is obtained using equation (1), where $t\phi$ is the time difference between the zero crossing points, described above, and T is signal time period.

$$\varphi = 2\pi \left| \frac{t_\varphi}{T} \right| \qquad (1)$$

Due to the difficulties associated with measuring phase differences close to and equal to zero using a pulse width generator the phase of V_2 is shifted by π radians. The output, V_{out} (mV), representing the impedance phase angle change is therefore calculated using equation (2), where V_{max} is the output corresponding to a full voltage cycle.

$$V_{out} = (\pi + \varphi) \times \frac{V_{max}}{2\pi} \quad (2)$$

2.2 Impedance spectroscopy of cells

Endothelial cells (type ECV304) were seeded at the same concentration (2×10^5 cells/well) in each well in the two external rows of 12-well plates. The complete culture media used was Medium 199 with 25 mM HEPES, supplemented with 100 U/ml penicillin and 100 µg/ml streptomycin (1 % Pen/Strep), 2 mM L-glutamine and this media was completed with 10 % heat-inactivated foetal bovine serum (FBS) previously filtered (all from Sigma Aldrich, U.K.) pre-warmed at 37 °C before use.

The cell culture medium was changed 2 days after plating and cells were allowed to reach confluence, usually 4 days after plating. After confluence, the culture medium was removed from the culture using an aspirator and 1 ml of complete M199 medium containing increasing toxin concentrations was added to each well. Four concentrations of DMSO (0.5 %, 1.25 %, 2.5 % and 5 % (v/v), four concentrations cadmium chloride (1, 10, 50, and 100 µM) and four concentrations of saponin (0.5 µg/mL, 1 µg/mL, 2 µg/mL and 10 µg/mL) were studied. For control purposes, 1 ml of fresh complete medium without toxin was added to the control well in each 12-well plate. An impedance spectrum was recorded every 30 minutes for 24 hours. During measurement the 12-well plate and the impedance analyser were kept in the incubator to allow the cells to grow in normal conditions at 37 °C in a humidified atmosphere containing 5 % CO_2. The impedance data (phase change in mV) from each test well was corrected using the signal from the control well to give a difference spectrum in mV. Four replica measurements for each toxin concentration were performed. Culture media alone with and without toxin gave no difference in the impedance spectra (data not shown).

2.3 Data Analysis

An impedance difference spectrum (i.e. the output voltage, V_o, representing the phase change difference between test and control) was obtained for each cell culture well every 30 minutes over a period of 24 hours. The 3D impedance difference spectra spanned the range of frequencies from 400 kHz to 2400 kHz, measurement being performed at intervals of 10 kHz. The impedance difference spectra for each toxin were used to determine the linear correlation between the difference in output voltage (mV) and concentration. Correlation coefficients were calculated for concentration of toxins with respect to output measurements at every frequency and time interval. These correlation coefficients were used to plot a "toxin map" of coefficients at each frequency-time point. By using threshold values of +0.95 and -0.95, areas of positive (red) and negative (blue) correlation are identified indicating regions of significance. Areas above and below the threshold values are plotted to produce the toxin map. An example of a plot of the regression space, in which all the correlation coefficients are mapped against time and frequency, is shown in figure 2. Toxin maps for each of the three different toxins are shown in Section 3.0 below. Four toxin maps were generated for each toxin (one for each replica measurement).
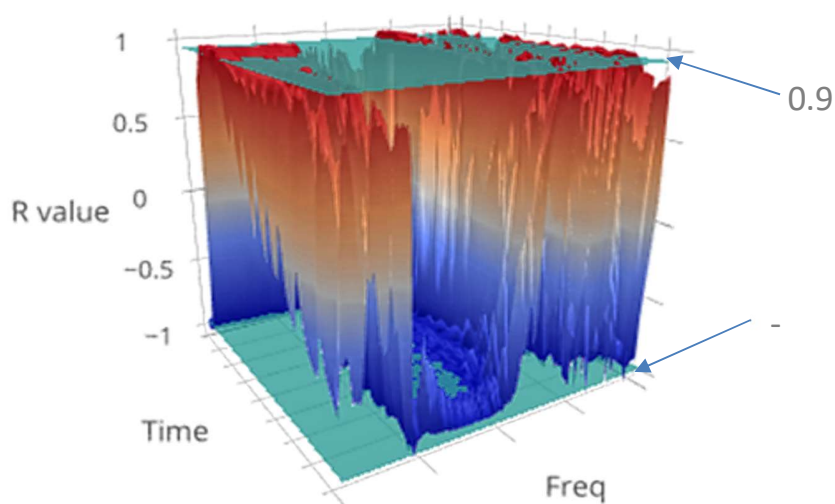
Fig. 2. The 3D impedance spectrum that represents the ECV304 cell effects to DMSO, obtained after subtraction of the output voltage from treated and control cells, and (B) Toxin map produced from the cell responses at four different DMSO concentrations, that represents points of correlation between cell effects and dose at 3 and 20 hours.

2.4 Cell size quantification by phase contrast microscopy

Phase-contrast microscopy of the ECV304 cells was performed after 24 hours exposure to toxins, in order to observe the changes in the cells as a result of the toxic challenge. The average cell size was calculated from 50-70 cell measurements in at least 3 different images. The size was determined after calibration of the software by the image of a haemocytometer chamber (magnification x 200). The data was expressed as the change of cell size (µm) of the treated cells minus the control cells. The average of triplicate measurements on control cells was used to determine the difference between the treated cell measurements and control cells.

2.5 Lactate Dehydrogenase (LDH) Assay

LDH is normally present in the cytoplasm of living cells and is released into the cell culture medium through leaky cell membranes of dead or dying cells that have been adversely affected by a toxic agent. In this study, small amounts of culture medium were removed at 3 hours and 24 hours after treatment of the cells to measure the amount of LDH released. The assay for LDH release was performed using Sigma LDH measurement kit. Cell supernatants from each of the 8 wells utilized in the 12 well plate were collected in 1.5 ml eppendorf tubes and centrifuged (250 g, 5 min) to remove cell debris. 100 µl aliquots of supernatant was dispensed into a 96-well microtiter plate and mixed with 50 µl/well of LDH substrate (containing diaphorase, NAD+, iodophenyl-nitrophenyl-phenyltetrazolium chloride and sodium lactate). The well plate was covered with foil to protect it from light and incubated at room temperature for 30 minutes. The reaction was stopped with 10 µl of 1M HCl added to each well. Plates were then read using a plate reader (Anthos Labtec Instruments, A-5022 Salzburg) at 490 nm using a reference wavelength of 685 nm. A background measurement at 685 nm was made to correct the endogenous absorbance of the complete medium and

used to correct all measurements made on the cells. A positive control was prepared by collecting the media from cells treated with 0.01 % saponin to lyse all the cells. All samples were triplicates. The percentage LDH leakage was calculated from the absorbance of the cells treated with toxins minus the absorbance of background, divided by the background corrected absorbance of the saponin positive control.

3.0 Results

The results of impedance measurements on confluent cultures ECV304 cells for the three toxins used in this study are presented in the form of toxin maps (The original 3D impedance data is provided as supplementary material figures S1, S3 and S5). Alongside the toxin maps, data associated with cell size, determined from phase contrast images (provided as supplementary material figures S2, S4 and S6) and LDH levels, demonstrating the integrity of the cell membranes are provided for each toxin at the four different concentration levels.

3.1 DMSO Treatment

3.1.1 DMSO Toxin Map

A toxin map for ECV304 cells treated with DMSO, shown in figure 3(A), was created from the 3D impedance spectra for the four concentrations of DMSO studied. The 3D impedance spectra are provided as supplementary material figures S1 (This is an example of the spectra produced from the 4 replica experiments.). The toxin map demonstrates large regions of positive and negative correlations. There was a greater than 85% concordance between the 4 replica experiments. A wide area of negative correlation is evident for approximately the first half an hour at high frequencies between approximately 1800 kHz and 2400 kHz, corresponding to the 'step region' seen in the 3D impedance spectra. This changes to positive correlation between approximately 3 and 8 hours and after this time very little correlation can be observed. There is a large area of negative correlations in the range from 1080 to 1800 kHz, corresponding to frequencies of the 'wave region' shown on the 3D impedance plots, in which a wave of peaks over this frequency range extend further in time as the concentration of DMSO increases. Over time the negative correlation changes from the lower end of frequency range of the 'wave region' to the higher end, remaining approximately constant between 1380 and 1800 kHz after about 8 hours. Between approximately 960 kHz and 1080 kHz there is a region of positive correlation up to approximately 5.5 hours, after this little correlation is observed. This could be related to the 3D spectra which show that there is little change in the output after 5.5 hours, indicating that the cells have been maximally effected by the toxin at this point. At frequencies below 960 kHz sporadic correlation can be identified, with correlation across the nearly whole experimental period at specific frequencies around 450 kHz, 470 kHz, 540 kHz and 820 kHz. The sporadic nature of this correlation data is consistent with the unstable impedance output shown at lower frequencies on the 3D impedance spectra in the supplementary material.

3.1.2 Cell size

The cell size increases with DMSO concentration, measured after 24 hours of incubation in DMSO, as shown in figure 3B. The Pearson's correlation coefficient (r) for the change in the cell size with increasing concentration of DMSO applied to the cells is 0.826. The average size difference of ECV304 cells, relative to the control cells, increased with the applied DMSO concentrations from 6.9 ± 10.4 µm with 0.5 % DMSO *(chi-square probability $X^2 < 0.05$)* to 76.2 ± 50.8 µm with 5 % DMSO, this increase in cell size was statistically significant *(p<0.01)*. This increase in cell size can be clearly seen in the phase contrast microscope image, provided in the supplementary material figure S2. It was noted that there was a wide distribution of cell size as some cells started to become enlarged at lower doses and at higher doses all the cells become enlarged but still display a wide range of cell size. This may indicate that individual cells respond to DMSO in slightly different ways, perhaps dependent on the phase of the cell cycle. Also it was noted that as the DMSO dose increased greater numbers of apoptotic cells were observed with 20% cell death at 24 hours.

3.1.3   LDH Release

The percentage of LDH released, relative to the positive control, at 3 and 24 hours of incubation in DMSO are shown in figure 3(C). At 3 hours ECV304 cells did not show a dose dependent release of LDH, but at 24 hours exposure to DMSO the release of LDH became dose dependent (p<0.01), 72.2 ± 15.4 % in ECV304 cells, rising to over 70% at 5% DMSO concentration.

The correlation coefficients for the percentage of LDH release at 3 hours and 24 hours were 0.365 and 0.832 respectively. The results imply that DMSO causes a low level of damage to the cell mechanisms maintaining cell membrane integrity at 3 hours, across all toxin concentrations. Whereas, after 24 hours, there is a significant dose dependent release of LDH due to loss of cell membrane integrity and cell death which is evident by the increasing numbers of apoptotic cells seen in the phase contrast image (available as supplementary material figure S2).
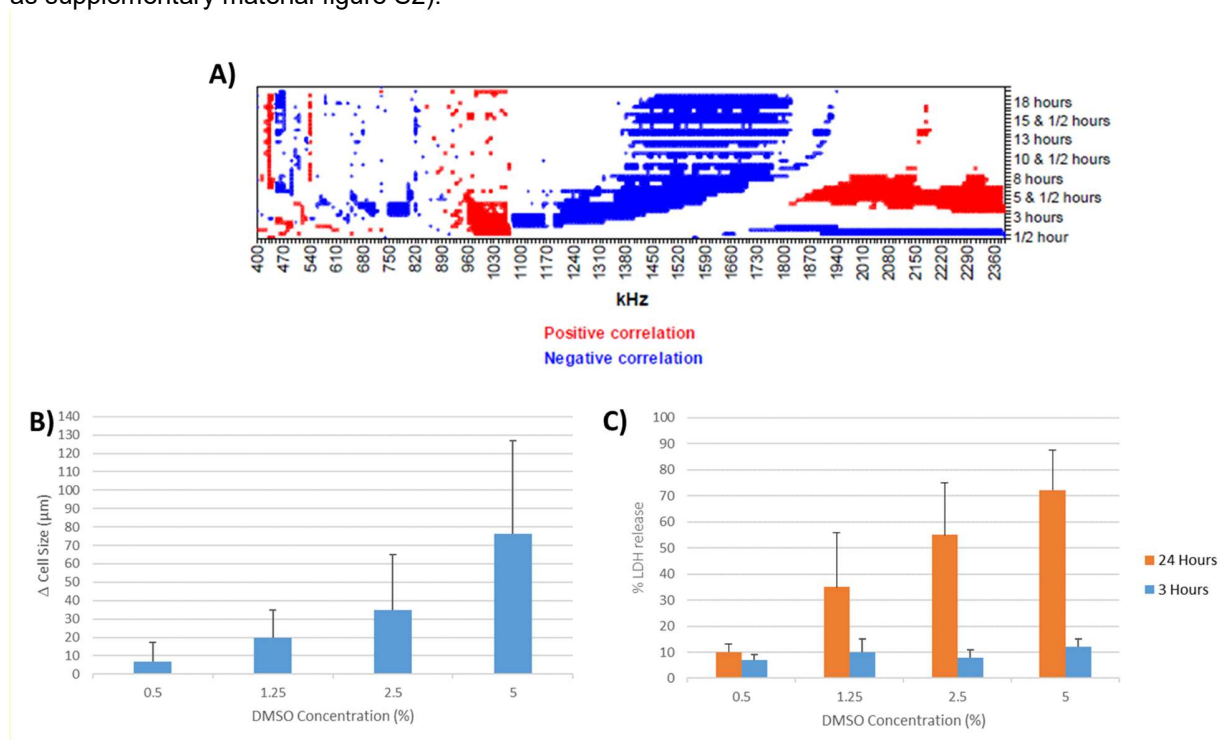

Fig. 3. A) Toxin map of ECV304 response to DMSO treatment during 24 hours at the frequency range 400-2400 kHz, B) Cell size (µm) dependence on DMSO toxin dose after 24 hours of toxin treatment of 0.5 %, 1.25 %, 2.5 %, and 5 %, C) LDH (%) release dependence on DMSO toxin challenge at 3hours and 24 hours exposure time.

3.2 Saponin Treatment

3.2.1   Saponin Treatment Toxin Map

The toxin map for ECV304 cells, treated with four concentrations of saponin, figure 4(A) shows mainly areas of positive correlation. The main area of correlation is approximately between 1080 kHz and 1330 kHz and extends throughout the whole of the 24 hour measurement period. This corresponds to negative voltage peaks in the central region of the 3D impedance plots (provided as supplementary material figure S3) that show a gradual increase in magnitude with increasing saponin concentration. At higher frequencies, there is a wide negative correlation band within the first two hours of saponin treatment and a positive correlation from approximately 3 to 8 hours. There is also evidence of this region in the 3D plots where a clear step between the mid frequency and the high frequency impedance outputs at approximately 1850 kHz can be distinguished. At lower frequencies between 430 and 440 kHz, there are isolated areas

of correlation at various frequencies. The sporadic nature of the correlation relating to the unstable impedance values at low frequencies, as discernible on the 3D impedance spectra provided in the supplementary material figure S3.

3.2.2 Cell size

Figure 4(B) shows a graph of average size of the ECV304 cells versus concentration of saponin after 24 hours incubation in saponin. The average change in cell size relative to the control increased with saponin concentration (r = 0.589) up to 39.7 ±31.5 µm with 10 µg/ml saponin as shown in figure 4B. This increase in size was statistically significant with saponin dose (p<0.05). The photomicrographs shown in the supplementary material figure S4 demonstrate that as the concentration of saponin increased, the morphological changes in ECV304 cells became more pronounced. Larger cells (arrow b) fused to form multinucleated cells (arrow c) at the higher concentrations of saponin. This increase in cell size is an expected result for cells exposed to saponin as its mode of action is to interact with cell membranes to form pores through which fluid is drawn into the cell due to osmotic pressure.

3.2.3 LDH Release

Exposure to increasing concentrations of relatively low doses of saponin causes some LDH release from the ECV304 cells compared with the control (p<0.05) as seen in figure 4(C). At the lower doses of saponin, up to 2 µg/ml, the dose had little effect on the release of LDH at 3 and 24 hours. But a dose of 10 µg/ml saponin caused a greater loss of LDH from the cell from 46.2 ± 7.8 % at 3 hours to 72.2 ± 34.7 % at 24 hours. This implies that there is a threshold dose above which saponin causes a significant increase in LDH loss as a results of a greater number of pores being formed exceeding the cells ability to compensate for lower levels of membrane damage. In addition, the higher number of apoptotic cells seen in the micrographs in the supplementary material figure S4 and the formation of large multinucleated cells (arrow c) can lead to release of LDH. 30% cell death was observed at 3 and 24 hours.
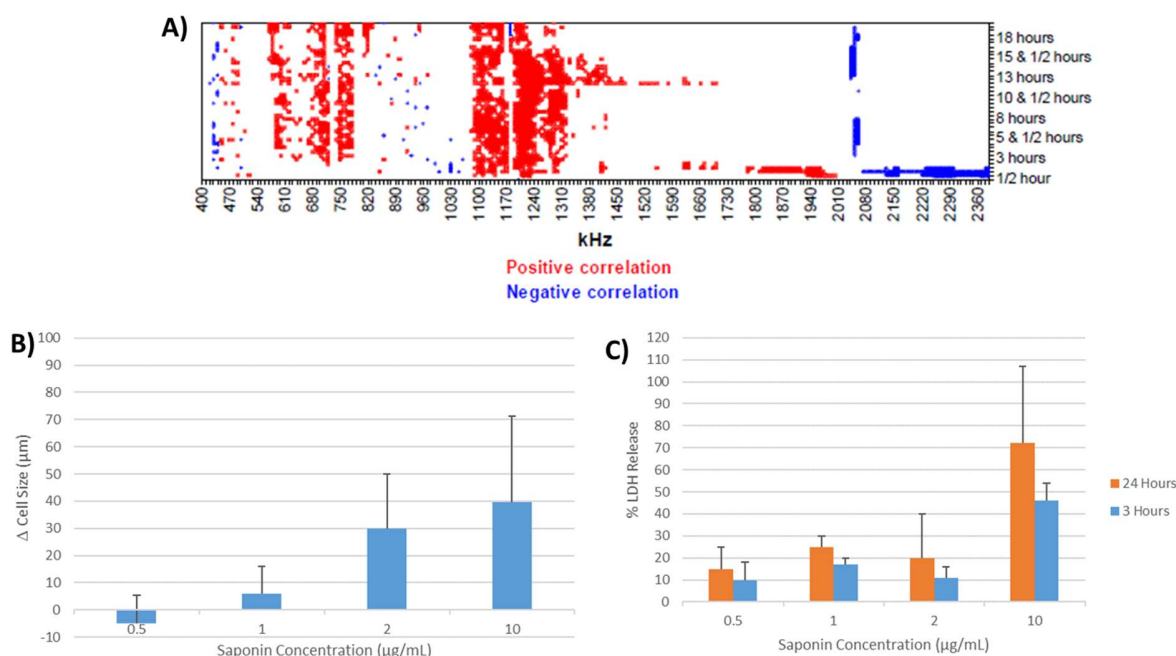

Fig. 4. A) Toxin maps of ECV304 response to Saponin treatment during 24 hours at the frequency range 400-2400 kHz, B) Cell size (µm) dependence on Saponin toxin dose performed after 24 hours of toxin treatment of 0.5 µg/mL, 1 µg/mL, 2 µg/mL, and C) LDH (%) release dependence on Saponin toxin challenge at 3 hours and 24 hours exposure time.

3.3 Cadmium Chloride Treatment

3.3.1   Cadmium Chloride Treatment Toxin Map

The cadmium chloride toxin map (figure 5(A)) shows a number of positive and negative bands of correlation. At lower frequencies there were a number of these, some well define, e.g. ~500 kHz and ~750 kHz for the total 24 hour measurement period and other bands were more sporadic up to approximately 1.1 MHz. At the higher frequencies there were two bands of positive correlation at approximately 1260 kHz and 2200 kHz. These frequencies, where correlation is found, appear to be related to the peaks of high impedance values which extended across the whole of the experimental period as is evident on the 3D impedance plots (provided in the supplementary material figure S5). The 3D plots also show that there was very little change in impedance values across most other frequencies in the spectrum, particularly in the mid-frequency measurement range. The higher frequency band at approximately 2200 kHz corresponds to the "step" feature observed on the 3D impedance plots.

3.3.2   Cell size

The average cell size increased significantly (p<0.01) when the cells were exposed to 50 µM concentration of cadmium chloride (0 ± 1.6 µm) or 100 µM cadmium chloride (10.7 ± 2 µm) as shown in figure 5(B). This would imply that the effect of cadmium chloride on the cells reached a limit at 50 µM. However, there was a trend for cells to shrink relative to the control cells with lower concentrations of cadmium chloride. The photomicrographs shown in the supplementary material figure S6 reveal larger cells at the higher cadmium chloride concentrations, but it can be seen that some cells are enlarged at 10 µM despite not seeing an overall increase in cell size. There are a few apoptotic cells visible at all cadmium chloride concentrations.

3.3.3   LDH Release

The percentage LDH release relative to the control was lower than that seen with the other two toxins, reaching a maximum of approximately 20% (figure 5(C)). Apart from 1 µM cadmium chloride exposure there was not a significant difference in the percentage LDH release after the 3 hour and 24 hour exposure. This implies that cadmium chloride exerts its effect on the cells within the first 3 hours of exposure at concentration of 10 µM and above. The lower levels of percentage LDH release and low number of apoptotic cell observed are consistent with only 5% cell death at 3 hours and 15% at 24 hours, lower than with the other toxins tested.
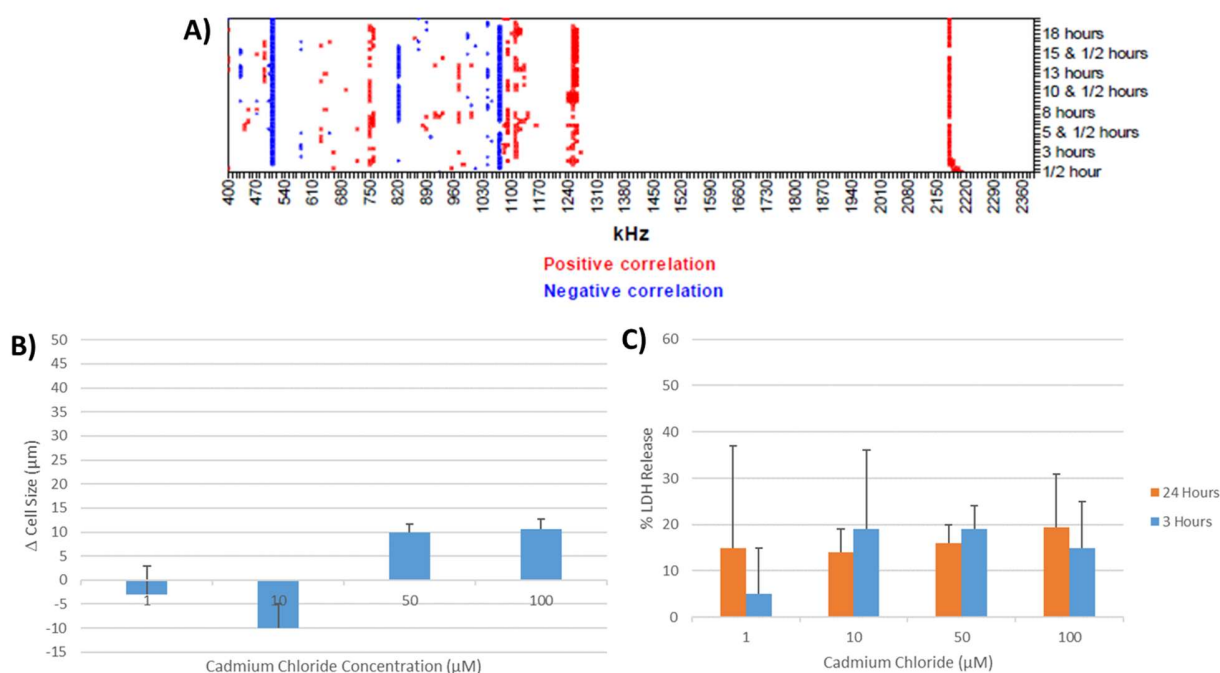
Fig. 5. A) Toxin maps of ECV304 response to cadmium chloride treatment during 24 hours at the frequency range 400-2400 kHz, B) Cell size (μm) dependence on Cadmium Chloride performed after 24 hours of toxin dose of 1 μM, 10 μM, 50 μM, and 100 μM, C) LDH (%) release dependence on Cadmium Chloride toxin challenge at 3hours and 24 hours exposure time.

4.0 Discussion

Impedance analysis within the beta dispersion region, i.e. the frequency range 10 kHz to 100 Mhz [23] has been shown to be optimum for evaluation of cellular activity in biological systems. Within this frequency range the cell membrane can be modelled as a parallel combination of capacitance and resistance, where the reactance of the membrane capacitance short circuits the membrane resistance, so the external electric field begins to penetrate into the cell interior. By comparison, in the alpha dispersion region, at frequencies below 10 kHz, the resistance of the cell membrane insulates the electric field from the cell interior. Within the study presented here, all measurements were recorded within the beta dispersion region.

A broadband approach to impedance measurement is required to investigate multiple cell properties [24]. In the model developed investigating the interaction between an electric field and a single cell [25], three frequency bands were defined; 0.8 – 2 MHz, 2 MHz – 12 MHz and 12 – 60 MHz. The high frequency band was associated with changes in the cell cytoplasm, the middle frequency band was associated with the cell membrane and the lower frequency band was related to the cell diameter. In a second model developed [26] also for a single cell, cell interactions were classified into 3 slightly different frequency bands; 0.1 – 10 KHz, 10 – 1 MHz, 1MHz to 10MHz. The high frequency band was associated with changes in the cytoplasm of the cell, while changes in the cell membrane were associated with mid (as well as the high) frequency bands. Finally, it was suggested that cell size could be associated with all frequency bands in their model, as there is clearly interdependency in the changes in size with both changes on cytoplasm and cell membrane.

Work reported in the literature [25, 26] is based on models and observations from experiments where the cells are in intimated contact with the electrodes and consequently the interpretations are related to this type of experimental design. In our system, the cells are grown in a standard tissue culture plate and are not in contact with the electrodes. Despite this difference in system design, it is reasonable to assume that there will be similarities in the frequency ranges associated with different cell properties. Based on the toxin maps created in this study, the frequency range can be divided into three approximate bands: 400 -1100 KHz; 1100 – 1800 KHz and 1800 -2400 KHz. Based on the frequency bands in the models described above and whilst noting the interdependency between the factors, it can be postulated that the lower frequency

band is broadly related to cell size, the mid-range band is related to cell membrane changes and the higher frequency band is related to changes in the cell cytoplasm.

All the toxin maps show areas of significant correlation in the low frequency band. Compared with the mid and high bands, this correlation tended to be more sporadic over the experimental period of 24 hours. This observation could be related to the 3D impedance spectra (provided in the supplementary material) in which the impedance values were less stable in the low frequency band compared with the mid and high frequency ranges. This implies that in the low frequency band, the impedance output is very sensitive to very slight changes in the cell system, for example due to changes in cell morphology as cells divide and grow, leading to a less consistent set of changes compared with the mid and high bands. The number of frequencies that showed correlation within the low frequency band was significantly less for cadmium chloride compared with saponin and DMSO. This was consistent with the cell size measurement from the phase contrast microscope images. A statistically significant increase in cell size was seen with all toxins applied. However, treatment with cadmium chloride resulted in a maximum of 10% change in cell size after 24 hours, whereas for saponin and DMSO a 40% and 75% change in cell size respectively was observed. Early in the test period within the low frequency band, DMSO had the greatest number of frequencies which showed correlations but many of these became more sporadic after approximately 5 hours. This may indicate that before 5 hours the DMSO starts to induce significant changes the cells (as observed in the change of cell size seen in the photomicrographs at 24 hours) and after 5 hours there was a less marked increase in the cell size for any of the concentrations studied.

In the mid-range frequency band of the toxin maps, both DMSO and saponin show large areas of correlation whereas for cadmium chloride there is a single, narrow band at 1260 kHz. It is postulated that changes in the cell membrane can are associated with changes in impedance in the mid-range frequency band. The release of LDH from the cell is a measure of the cell membrane integrity. Exposure to saponin and DMSO resulted in a maximum of 72% LDH release, relative to the control, at 24 hrs and showed significant correlation with dose. Both saponin and DMSO had areas of positive correlation between 1100 and 1300 kHz. In contrast, exposure to cadmium chloride did not result in a significant dose response, with a maximum LDH release of 20% at 24 hrs. For the DMSO the dose dependence of LDH release at 24 hours was clear, whereas at 3 hours the correlation coefficient was low. This implies that the majority of DMSO induced damage to the cell membrane occurs after three hours.

The high frequency regions of the toxin maps, which we propose is related to internal cell structures, showed areas of correlation for all three toxins. DMSO showed the greatest area of correlation, both negative and positive. Whereas, with cadmium chloride, a narrow band of positive correlation is seen around 2190 kHz and, with saponin, a narrow band of negative correlation is seen around 2060 kHz along with a wide band of negative correlation up to 2400 kHz for the first 2 hours of exposure. This implies that DMSO is a broad acting toxin that exerts its toxic affect in a dose dependent manner over the first 8 hours of exposure. The narrow band of correlation seen with cadmium chloride and saponin indicate a more specific effect on the internal cell structure. This is the case with saponin which affects primarily the cell membrane. Impedance measurements themselves do not give information of specific processes, but could indicate particular areas of the cell anatomy and metabolism that are affected by a toxin.

For all toxins significant dose dependent changes in the impedance spectra could be seen within 30 minutes of exposure to the toxin. In this study the first measurement point occurred 30 minutes after each toxin was added. Consequently, it was probable that dose dependent changes were happening before this time point.

Further work is required to identify differences in the toxin maps associated with a broader range of toxins. It is hypothesized that similar patterns of correlation will indicate similar modes of toxicity to a given cell. Given an unknown toxin we are able to classify the cytotoxic mode-of-action from the toxin map, but would not be able to identify the specific compound. In principle, with a complex solution of toxins we would expect to see a summation of the toxin maps of the different modes of action, but this has not yet been assessed. Impedance measurements themselves alone do not give information of specific cellular processes, but do indicate particular areas of the cell anatomy and metabolism that are affected by a toxin challenge. We may apply other conventional validation techniques to assess cytotoxicity to evaluate inhibition of some important pathways to correlate with our impedimetric data. Conventional cytotoxicity assays rely on measuring one or more cytotoxic indicators. We could assess loss of membrane apoptosis by activation of caspases. In the case when toxicity occurs without membrane damage, ATP depletion, and GSH depletion potentially could be measured.

Our system recorded impedance spectra every 3 minutes over a total time period of 24 hours, detecting morphological changes in the cells due to toxins in real-time. These changes involve molecular mechanisms starting with membrane proteins signaling followed by morphological changes and ending with cell death. Similarly cell proliferation may be detected by our method of impedance spectroscopy to establish cell division generation time.

Given an unknown toxin we are able to classify the cytotoxic mode-of-action from the toxin map, but would not be able to identify the specific compound. In principle, with a complex solution of toxins we would expect to see a summation of the toxin maps of the different modes of action, but this has not yet been assessed.

Our system could be applied to sense morphological changes in other cell types [18], including bacteria cells. One of the primary components of the bacterial cell wall is peptidoglycan, a structural macromolecule with a net-like composition that provides rigidity and support to the outer cell wall. Throughout a bacterial lifecycle, the cell wall (and thus the peptidoglycan crosslinks) is continuously remodeled in order to accommodate for repeated cycles of cell growth and replication. Thus, in principle we would be able to identify frequency bands in a toxin map that reflect these changes and also changes due to addition of drugs, such as penicillin. Penicillin and other antibiotics in the beta-lactam family contain a characteristic four-membered beta-lactam ring. Penicillin kills bacteria through binding of the beta-lactam ring to DD-transpeptidase, inhibiting its cross-linking activity and preventing new cell wall formation. It is concluded from our results that the mid-range frequency band 1100 – 1800 KHz is related to changes to the cell membrane. This is in concordance with other reported EIS systems, developed [27] to detect and enumerate bacteria in water samples. Furthermore, it is reported [27] that it is possible to differentiate between gram positive and gram negative bacteria. The author [27] suggested higher frequencies in the range 1MHz to 10MHz are capable of partially penetrating the membrane of the bacteria and thus probe the membrane and cytoplasm composition.

5.0 Conclusions

In this study, we developed a real-time, non-contact impedance spectroscopy measurement and analysis technique for cytotoxicity testing. The analysis involves the creation of a 'toxin map' in which the correlation factor between the impedance of a culture of endothelial cells (cell line ECV304) and toxin dose is plotted with respect to input signal frequency and time. The results demonstrated that each toxin generated a characteristic toxin map, with the four replica experiments for each toxin demonstrating greater than 85% concordance. Moreover, the maps for each of the three toxins demonstrated significant differences, which could be related to the differing modes-of-action of the toxin on the cells. For example, the broad acting toxin, DMSO, showed many areas of correlation across mid and high frequencies in the measurement range (400 kHz to 2400 kHz), whereas cadmium chloride showed correlation only in a few narrow frequency bands, which was commensurate with the specific action of cadmium chloride in the cell, for example binding with membrane targets to inhibit calcium channels.

Future work will focus on determining the association of cell changes with regions of correlation on a toxin map. This can be achieved by evaluating toxins that have well characterized, specific modes of action. In addition, impedance measurements will be performed every minute after the addition of the toxin in order to establish how quickly characteristic patterns can be created. The technique presented shows potential for application in high throughput screening as it permits real-time, non-contact monitoring of the cells and rapidly provides characteristic outputs dependent on the toxin.

Author contributions

Richard Luxton and Janice Kiely conceived the original concept, funding acquisition and provided supervision and resources. Angelines Gasser contributed to the methodology, carried out the investigation and initial analysis of the data. John Eveness wrote the original draft of the manuscript and contributed to visualization and interpretation. Janice Kiley, Richard Luxton and David Attwood reviewed and edited the draft and sanctioned the final version of the manuscript.

Appendix A. Supplementary material

References

[1] Xu, Y., Xie, X., Duan, Y., Wang, L., Cheng, J., Cheng, Z., A review of whole cells, Biosensors and Bioelectronics. 77 (2016) 824-836.

[2] Zhang, X., Li, F., Nordin, A.N., Tarbell, J., Voiculescu, I., Toxicity studies using mammalian cells and impedance spectroscopy method, Sensing and Bio-Sensing Research. 3 (2015) 112-121.

[3] Thakur, M., Mergel, K., Weng, A., Frech, S., Gilabert-Oriol, R., Bachran, D., Melzig, M.F., Fuchs, H., Real time monitoring of the cell viability during treatment with tumor-targeted toxins and saponins using impedance measurement, Biosensors and Bioelectronics. 35 (2012) 503-506.

[4] Primiceri, E., Chiriacò, M.S., D'Amone, E., Urso, E., Ionescu, R.E., Rizzello, A., Maffia, M., Cingolani, R., Rinaldi, R., Maruccio, G., Real-time monitoring of ion-induced cytotoxicity by EIS cell chips, Biosensors and Bioelectronics. 25 (2010) 2711-2716.

[5] F. Sambale, S. Wagner, F. Stahl, R. R. Khaydarov, T. Scheper, D. Bahnemann, Investigations of the Toxic Effect of Silver Nanoparticles on Mammalian Cell Lines, Journal of Nanomaterials. 136765 (2015) 1-9.

[6] Schneider, D., Tarantola, M., Janshoff, A., Dynamics of TGF-β induced epithelial-to-mesenchymal transition monitored by electric cell substrate impedance sensing, Biochimica et biophysica acta. (2011) 1813 2099.

[7] Parekh, A., Das, D., Das, S., Dhara, S., Biswas, K., Mandal, M., Das, S., Bioimpedimetric analysis in conjunction with growth dynamics to differentiate aggressiveness of cancer cells, Scientific reports. 8 (2018) 783-10.

[8] Gamal, W., Borooah, S., Smith, S., Underwood, I., Srsen, V., Chandran, S., Bagnaninchi, P.O., Dhillon, B., Real-time quantitative monitoring of hiPSC-based model of macular degeneration on Electric Cell substrate impedance sensing microelectrodes, Biosensors and Bioelectronics. 71 (2015) 445-455.

[9] Wang, L., Yin, H., Xing, W., Yu, Z., Guo, M., Cheng, J., 2010. Real-time label free monitoring of the cell cycle cellular impedance sensing chip, Biosensors and Bioelectronics. 25 (2010) 990-995.

[10] Diemert, S., Dolga, A.M., Tobaben, S., Grohm, J., Pfeifer, S., Oexler, E., Culmsee, C., Impedance measurement for real time detection of neuronal cell death, Journal of Neuroscience Methods. 203 (2012) 69-77.

[11] Benson, K., Cramer, S., Galla, H., Impedance-based cell monitoring: barrier properties and beyond, Fluids and barriers of the CNS. (2013) 10, 5.

[12] Lundstrom, K., Cell-impedance-based label-free technology for the identification of new drugs, Expert opinion on drug discovery. 12 (2017) 335-343.

[13] Andrew R Collins, High throughput toxicity screening and intracellular detection of nanomaterials, Nanomedicine and nanobiotechnology. 9 (2017) 1-30.

[14] Del Peso, A., Repetto, G., Zurita, J.L., Natural red uptake assay for the estimation of cell viability/cytotoxicity, Nature Protocols. 3 (2008) 1125-1131.

[15] Djawad, Y.A., Attwood, D., Kiely, J., Luxton, R., The application of detrended fluctuations analysis to assess physical characteristics to the human cell line ECV304 following toxic challenges, Sensing and Bio-Sensing Research. 23 (2019) 100269.

[16] Djawad, Y., Kiely, J., Nibouche, M., Wraith, P., Luxton, R., Robust feature extraction from impedimetric signals using wavelet packet decomposition with application to cytotoxicity testing, IET Science, Measurement & Technology. 6 (2012) 456.

[17] Marimuthu, M., Park, C., Kim, S., Choi, C.S., Real-time electrical measurement of L929 cellular spontaneous and synchronous oscillation, International journal of nanomedicine. 7 (2012) 83-92.

[18] Wang, Z., Zhu, Q., Kiely, J., Luxton, R., Hilbert Huang Transform Impedance Measurement Data for Cellular Toxicity Monitoring, Proceedings of the 2009 IEEE International Conference on Networking, Sensing and Control, Okayama, Japan, March 26-29, 2009

[19] Wang, Z., Kiely, J., Luxton, R., Non-linear data analysis of impedance spectroscopy as applied to cellular toxicity systems, ICMIC. (2012) 1256-1262.

[20] Wang, Z., Kiely, J., Vargas, A.M., Luxton, R., Comparison of Cytotoxic Changes in ECV304 Cell Through Exposure to DMSO and Sodium Butyrate Using Impedance Spectroscopy, Procedia Chemistry. 6 (2012) 89-99.

[21] Cao, L., Kiely, J., Piano, M., Luxton, R., A Copper Oxide/Zinc Oxide Composite Nano-Surface for Use in a Biosensor, Materials (Basel, Switzerland). 12 (2019) 1126.

[22] Cao, L., Kiely, J., Piano, M., Luxton, R., Facile and inexpensive fabrication of zinc oxide based bio-surfaces for C-reactive protein detection, Scientific reports. 8 (2018) 12687-9.

[23] Grimnes, S., Martinsen, ØG., Alpha-dispersion in human tissue, Journal of Physics: Conference Series. 224 (2010) 012073.

[24] WenLai, T., DeZhi, T., ZhongHua, N., Nan, X., Hong, Y., A portable single-cell analysis system integrating hydrodynamic trapping with broadband impedance spectroscopy, Sci. China Technol. Sci. 60 (2017) 1707-1715.

[25] Sun, T., Green, N.G., Morgan, H., Analytical and numerical modelling methods for impedance analysis of single cells on-chip, Nano. 3 (2008) 55-63.

[26] Ren, D., Chui, C.O., Feasibility of Tracking Multiple Single-Cell Properties with Impedance Spectroscopy, ACS sensors. 3 (2018) 1005-1015.

[27] Clausen, C., Dimaki, M., Bertelsen, C., Skands, G., Rodriguez-Trujillo, R., Thomsen, J., Svendsen, W., Bacteria Detection and Differentiation Using Impedance Flow Cytometry, Sensors. 18 (2018) 3496.